FEBS Letters 587 (2013) 620–624

journal homepage: www.FEBSLetters.org

Interaction between soluble Aβ-(1–40) monomer and Aβ-(1–42) fibrils probed by paramagnetic relaxation enhancement

Takahiro Yamaguchi, Katsumi Matsuzaki, Masaru Hoshino *

Graduate School of Pharmaceutical Sciences, Kyoto University, 46-29 Yoshida-Shimoadachi, Sakyo-ku, Kyoto 606-8501, Japan

ARTICLE INFO

Article history:
Received 17 October 2012
Revised 26 January 2013
Accepted 4 February 2013
Available online 15 February 2013

Edited by Jesus Avila

Keywords:
Nuclear magnetic resonance
Paramagnetic relaxation enhancement
Cross seeding
Amyloid fibril
Dock-Lock model

ABSTRACT

The most common isoforms of amyloid-β (Aβ) proteins are composed of 40 or 42 amino acid residues. While Aβ-(1–40) is the predominant species, Aβ-(1–42) is more fibrillogenic and neurotoxic, suggesting that Aβ-(1–42) plays a critical role in the initiation of amyloid fibril formation. We investigated the mechanisms by which soluble Aβ-(1–40) associates with preformed Aβ-(1–42) seeds. A paramagnetic relaxation enhancement analysis showed that the Aβ-(1–40) monomer and Aβ-(1–42) seed interact via their C-terminal region in a parallel fashion, and the N-terminal part does not to contribute to the interaction.

Structured summary of protein interactions:
A beta-(1–40) and **A beta-(1–42)** bind by fluorescence technology (View interaction)
A beta-(1–42) and **A beta-(1–40)** bind by nuclear magnetic resonance (View interaction)

© 2013 Federation of European Biochemical Societies. Published by Elsevier B.V. All rights reserved.

1. Introduction

The aggregation and deposition of amyloid β-peptide (Aβ) are considered critical to the development of Alzheimer's disease (AD) [1,2]. The most common isoforms of Aβ are Aβ-(1–40) and Aβ-(1–42). Although Aβ-(1–40) is the predominant species, Aβ-(1–42) is more fibrillogenic and neurotoxic [3,4], suggesting that Aβ-(1–42) plays a critical role in the initiation of plaque formation and AD onset.

The most convincing model for the formation of amyloid fibrils is the nucleation-dependent polymerization model, which separates the fibrillization process into a nucleation phase and an elongation phase [5–8]. Nucleation requires the self-association of soluble monomers, which is thermodynamically unfavorable, resulting in a long lag-phase in the kinetics of amyloid fibril formation. Once the nucleus is formed, however, the further addition of monomers is a much more favorable process, and proceeds rapidly. Whereas fibril elongation is well approximated by a first-order kinetic model [7,8], a more detailed mechanism such as the Dock-Lock model is also proposed [9]. In this model, the soluble monomer first binds to the fibril terminus reversibly (the Dock-phase), and then the docked protein undergoes irreversible conformational change (the Lock-phase) to adopt the fibril structure. However, analysis of the fibrillization process is hampered by the short lifetime of the transiently attached molecule at the terminus of the fibrils.

In this study, we investigated the interaction between Aβ-(1–40) monomers and preformed Aβ-(1–42) fibrils. When preformed Aβ-(1–42) fibrils were added to soluble Aβ-(1–40) monomers, the growth of amyloid fibrils proceeded after a long lag period (~1 h). This enableed us to examine the site of interaction at the amino acid level using paramagnetic relaxation enhancement (PRE)-NMR measurements. We introduced the nitroxide radical MTSL at two different positions of Aβ-(1–42). When the MTSL spin-label was introduced at the N-terminal position of Aβ-(1–42) seed, the NMR peak intensity of soluble ^{15}N-Aβ-(1–40) did not change significantly. In contrast, when the spin-label was introduced at Ala30 of Aβ-(1–42) seed, a dramatic decrease in peak intensity was observed especially in the C-terminal region of soluble ^{15}N-Aβ-(1–40). These results demonstrate that the Aβ-(1–40) monomer and Aβ-(1–42) seed interact mainly via their C-terminal region.

2. Materials and methods

2.1. Materials

^{15}N-Ammonium chloride and sodium 2,2-dimethyl-2-silapentane-5-sulfonate (DSS) were purchased from SI Science Co. Ltd. (1-Oxyl-2,2,5,5-tetramethyl-Δ3-pyrroline-3-methyl)

Abbreviations: AD, Alzheimer's disease; Aβ, amyloid-β peptide; HSQC, heteronuclear single-quantum coherence; MTSL, (1-oxyl-2,2,5,5-tetramethyl-Δ3-pyrroline-3-methyl) methanethiosulfonate; NMR, nuclear magnetic resonance; PRE, paramagnetic relaxation enhancement

* Corresponding author. Fax: +81 75 753 4529.
E-mail address: hoshi@pharm.kyoto-u.ac.jp (M. Hoshino).

0014-5793/$36.00 © 2013 Federation of European Biochemical Societies. Published by Elsevier B.V. All rights reserved.
http://dx.doi.org/10.1016/j.febslet.2013.02.008

methanethiosulfonate (MTSL) was obtained from Toronto Research Chemicals. Other reagents were purchased from Nacalai Tesque.

2.2. Protein preparation

Expression and purification of non-labeled and uniformly ^{15}N-labeled Aβ-(1–40) were performed as described previously [10,11]. The plasmids encoding Aβ-(1–42) and mutant proteins, in which Ala2 or Ala30 was replaced by Cys, were constructed by the QuickChange (Stratagene) method using pET28a–H6UbAβ-(1–40) as a template DNA. Expression and purification of wild-type and mutant Aβ-(1–42) were performed with the same methods as for Aβ-(1–40), except for the reversed-phase HPLC conditions. The cleaved Aβ-(1–42) moiety was purified by using a $5C_{18}$-MS-II packed column (Nacalai Tesque, Kyoto, Japan) under alkaline conditions [12]. The fraction containing Aβ-(1–42) was collected and lyophilized.

Purified A2C-Aβ-(1–42) or A30C-Aβ-(1–42) was dissolved in 95% dimethyl sulfoxide/1% trifluoroacetic acid and a fivefold molar excess of MTSL was added to the solution. After a 1 h incubation at 25 °C, spin-labeled proteins were purified by HPLC. The purity and identity of the proteins were confirmed by reversed-phase HPLC and electrospray ionization mass spectrometry. The purity of the proteins was greater than 95%.

2.3. Seed-free preparation

Purified Aβ was dissolved in 0.02% ammonia on ice, and any large aggregates which could act as a seed for aggregation were removed by ultracentrifugation in polyallomer tubes at 540 000×*g*, 4 °C for 3 h. A supernatant fraction was collected, and the concentration of protein was determined in triplicate by Micro BCA protein assay (Pierce, Rockford, IL). The supernatant was stored as a stock solution at −80 °C prior to use.

2.4. Thioflavin T fluorescence

The protein stock solutions dissolved in 0.02% ammonia were mixed with the same volume of double concentrated PBS (16.0 g/l of NaCl, 0.40 g/l of KCl, 2.30 g/l of Na_2HPO_4 and 0.40 g/l of KH_2PO_4, pH 7.4) on ice, and further diluted by PBS to prepare a 15 μM sample solution. The sample temperature was raised to 37 °C to initiate the fibril formation. The sample (final Aβ concentration, 0.5 μM) was added to a 5 μM ThT solution in 50 mM glycine–NaOH buffer, pH 8.5. Fluorescence at 490 nm was measured at an excitation wavelength of 446 nm at 25 °C [8]. To prepare the seeds for the amyloid fibrils, spontaneously formed aggregates were sonicated on ice with 20 intermittent pulses (pulse of 0.6 s, interval of 0.4 s, output level of two) using an ultrasonic disruptor equipped with a TP-030 microtip (UD-201, Tomy, Tokyo). Sonicated seed fibrils at 5% (w/w) were added to seed-free Aβ.

2.5. Preparation of spin-labeled Aβ-(1–42) seed fibrils

Spin-labeled Aβ-(1–42) was incubated with wild-type Aβ-(1–42) seeds and the sample solution was incubated at 37 °C. Formation of amyloid fibrils was confirmed by ThT assay. The fibrils were collected by centrifugation (22 000×*g*, 10 min) and washed with water twice. The fibril suspension was sonicated as described above.

2.6. NMR measurements

NMR spectra were measured on a Bruker DMX600 spectrometer equipped with a triple-axis gradient TXI probe. Seventy-five micromolar of ^{15}N-labeled Aβ-(1–40) was dissolved in 50 mM sodium phosphate (pH 6.5), 100 mM NaCl, and 10% D_2O. ^{1}H–^{15}N HQSC spectra of ^{15}N-Aβ-(1–40) were measured at 25 °C in the absence or presence of 75 μM (monomer equivalent) spin-labeled Aβ-(1–42) seed fibrils. ^{1}H–^{15}N HSQC assignments were obtained previously [11]. The number of scans was eight and measurement time was approximately 40 min. The chemical shift value was referenced with DSS. The spectra were processed with nmrPipe and analyzed with nmrDraw and PIPP [13,14].

3. Results and discussion

3.1. The elongation kinetics of Aβ-(1–40) from Aβ-(1–42) seeds exhibits a lag phase

To elucidate the role of Aβ-(1–42) in Aβ aggregation, we analyzed the growth kinetics of the amyloid fibrils formed by soluble Aβ-(1–40) seeded with preformed Aβ-(1–40) or Aβ-(1–42) fibrils (Fig. 1). When the preformed Aβ-(1–40) seed was added to the soluble monomer of Aβ-(1–40), fibril elongation proceeded rapidly without a lag phase. In contrast, when the Aβ-(1–42) seed was added to Aβ-(1–40), the kinetic profile of fibril growth exhibited a sigmoidal shape with an apparent lag time (∼1 h). This implies that a subtle but significant difference between molecular species results in the slow extension kinetics and exhibits as the apparent lag phase. Similar results were obtained in other studies [15–17]. The results indicate that the Aβ-(1–40) monomer reversibly binds to the end of the Aβ-(1–42) seed during the lag phase, then becomes irreversibly associated after a conformational change as in the Dock-Lock model [9].

3.2. Interaction between the Aβ-(1–40) monomer and Aβ-(1–42) seed probed by PRE

The presence of a lag phase before the fibril growth prompted us to explore the interaction between the Aβ-(1–40) monomer and Aβ-(1–42) seed using PRE-NMR measurements. ^{1}H–^{15}N HSQC spectra of ^{15}N-Aβ-(1–40) were measured in the absence and presence of the seeds of amyloids formed by the spin-labeled

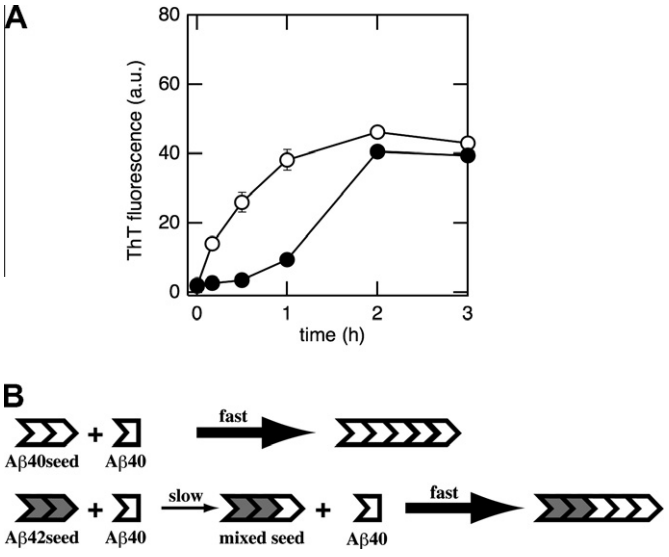

Fig. 1. (A) Analysis of cross-seeding activity of Aβ-(1–42). Seeds were prepared by sonicating spontaneously formed aggregates of Aβ-(1–40) (open circle) and Aβ-(1–42) (closed circle) and were added at 5% (w/w) to seed-free Aβ-(1–40) solution. After various incubation periods at 37 °C, an aliquot of sample was analyzed using ThT fluorescence. (B) A schematic drawing of cross-seeding experiment. A subtle but significant difference in molecular structure resulted in a slow binding kinetics, which exhibits as a lag-phase.

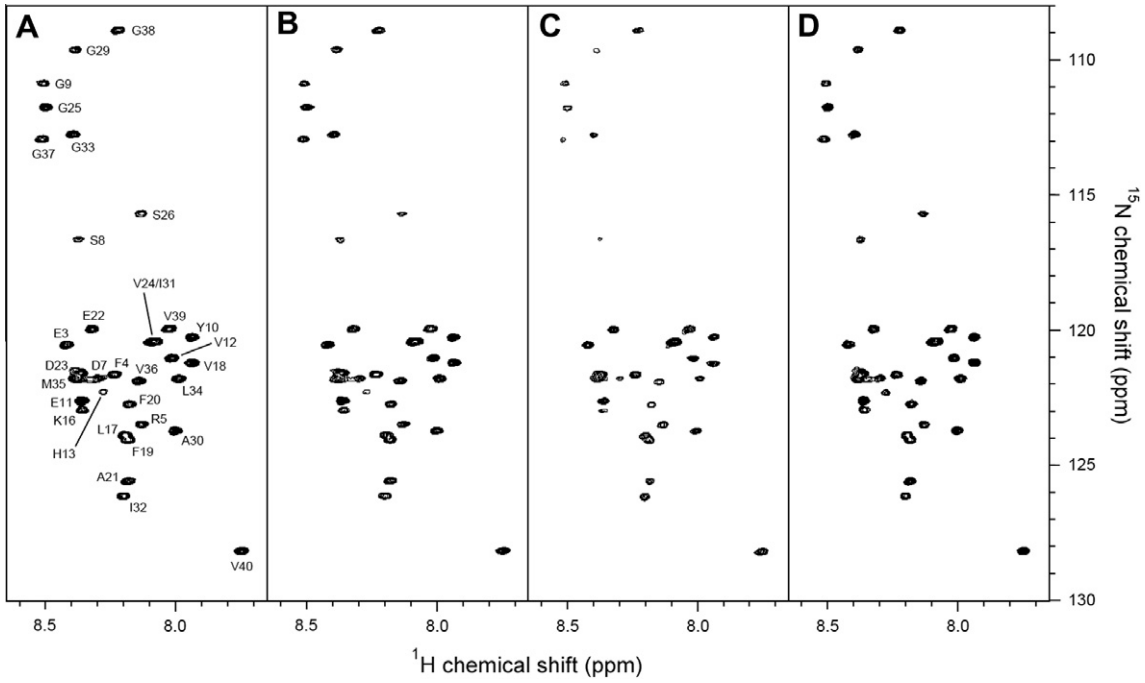

Fig. 2. ^{1}H–^{15}N HSQC spectra of ^{15}N-Aβ-(1–40) in the absence (A) and presence of seeds formed by spin-labeled A2C-Aβ-(1–42) (B), spin-labeled A30C-Aβ-(1–42) (C), or non-labeled A30C-Aβ-(1–42) (D). Seventy-five micromolar of ^{15}N-Aβ-(1–40) was dissolved in 50 mM sodium phosphate (pH 6.5), 100 mM NaCl, and 10% D_2O. ^{1}H–^{15}N HQSC spectra of ^{15}N-Aβ-(1–40) were measured at 25 °C in the absence or presence of 75 μM (monomer equivalent) Aβ-(1–42) seed.

Aβ-(1–42) at different positions (Fig. 2). In the presence of A2C-labeled seeds, the signal intensity was slightly and uniformly decreased to about 80% (Fig. 3, open circle). Similarly, a slight decrease in intensity was observed in the presence of unlabeled Aβ-(1–42) seeds (Figs. 2D and 3, closed triangle), indicating that the signal decrease caused by the A2C-labeled seeds is not due to the PRE-effect. The decrease might be due to the chemical exchange line broadening caused by the reversible binding and release events that occurred at the terminus of the amyloid fibrils.

In contrast, in the presence of A30C-labeled seeds, a significant decrease in peak intensity was observed (Fig. 3, open triangle). While the peak intensity change of N-terminal region was moderate (50–70%), a more dramatic decrease (~40%) was observed from the center to the C-terminal region, except for G38 and V39 whose relative intensities were ~60%. These results showed that the Aβ-(1–40) monomer and Aβ-(1–42) seed interact mainly via their C-terminal region.

In the present study, NMR spectra were measured in the presence of 75 μM (monomer-equivalent) of Aβ-(1–42) seeds. Since sonicated fibril seeds are thought to consist of at least 140 molecules [18], the concentration of the "active" ends of seed is considerably low (<0.5 μM). By introducing MTSL-labeling into A30C-Aβ-(1–42), the interaction with such low-populated species could be effectively detected because unpaired electrons dramatically increase the transverse relaxation rate of nearby (~25 Å) nuclear spins.

3.3. Effects of residual Aβ-(1–42) monomer on NMR signal intensity were negligible

Although the growth of amyloid fibrils is a strongly favorable process and proceeds almost irreversibly, a trace amount of soluble monomer should coexist with fibrils at the end of the reaction depending on the value of association and dissociation constants [19]. Furthermore, several groups have shown that Aβ-(1–40) and Aβ-(1–42) interact with each other in monomeric form [15–17,20]. Spin-labeled Aβ-(1–42) fibrils were collected by centrifugation and washed with water twice, however, some

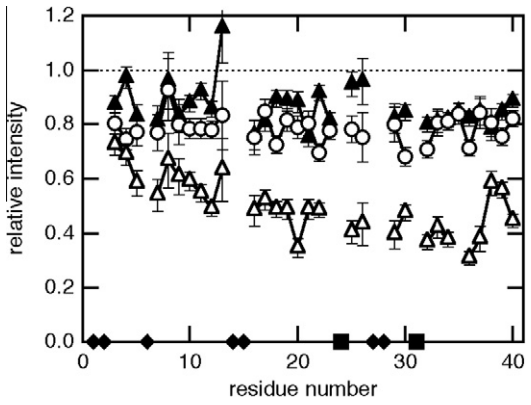

Fig. 3. Peak intensity of ^{15}N-Aβ-(1–40) in the presence of spin-labeled A2C-Aβ-(1–42) seeds (open circle), spin-labeled A30C-Aβ-(1–42) seeds (open triangle), or non-labeled A30C-Aβ-(1–42) seeds (closed triangle) relative to that in the absence of seeds. Closed diamonds show amino acid residues that were not observed at 25 °C. Overlapping peaks, V24 and I31, are indicated by closed squares.

soluble monomer still may coexist with the seed and the released spin-labeled monomer could affect the NMR signal intensity via non-specific random collisions with ^{15}N-Aβ-(1–40). To confirm that the observed decrease in signal intensity was caused by the interaction with the terminus of the fibrils and not with the released soluble monomer, the effect of the presence of the spin-labeled Aβ-(1–42) monomer on NMR signal intensity was investigated.

We first quantified the concentration of coexisting monomer with spin-labeled fibrils. The supernatant fraction after centrifugation of fibrils was analyzed by reversed-phase HPLC (Fig. 4). A standard calibration curve was prepared from the peak area of spin-labeled Aβ-(1–42) monomer of known concentration, and showed good linearity in the 0.5–5 μM concentration range (Fig. 4, inset). The concentration of the residual monomer in the seed sample was determined to be 0.996 μM. Next, ^{1}H–^{15}N HSQC

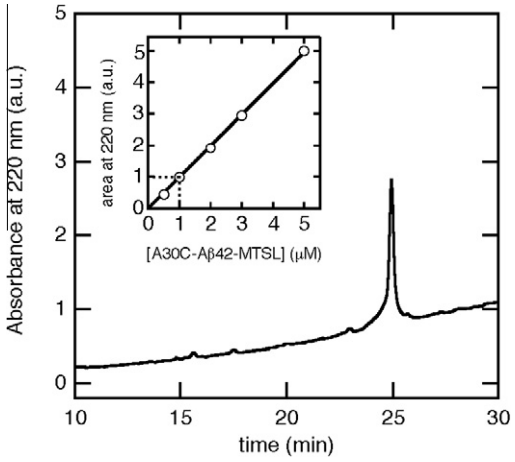

Fig. 4. Estimation of residual monomer concentrations in seed samples of spin-labeled A30C-Aβ-(1–42). Five-hundred microliters of supernatant fraction after centrifugation of spin-labeled fibrils was analyzed by HPLC. (Inset) The standard calibration curve prepared from the peak area of known concentration of spin-labeled A30C-Aβ-(1–42) monomer. The peak area and the corresponding concentration of the residual monomer are shown by a dotted line.

spectra of ^{15}N-Aβ-(1–40) were measured in the absence or presence of the 1 μM of spin-labeled A30C-Aβ-(1–42) monomer (Fig. 5). Although a slight and uniform decrease in peak intensity was observed (~90%), the effect of the residual monomer was almost negligible. This demonstrates that the significant decrease in peak intensity observed in the presence of spin-labeled A30C-Aβ-(1–42) seed is resulted from the interaction with the preformed fibril seeds.

3.4. Aβ-(1–40) monomer associates with Aβ-(1–42) fibrils in a parallel fashion

Recent studies with solid-state NMR spectroscopy suggest that the amyloid fibrils formed by Aβ-(1–40) and Aβ-(1–42) are predominantly composed of in-register, parallel β-sheets although several variations in molecular organizations have been identified [21–23]. These models of amyloid fibril of Aβs indicate in common that A30 is considered to be situated in the C-terminal β-strand. The present results indicated that while the Aβ-(1–40) monomer and Aβ-(1–42) seed interact through their C-terminal region, whereas the N-terminal residues were not involved. The similar results that demonstrating the flexible N-terminal regions is obtained by H/D exchange experiment of Aβ-(1–40) amyloid fibrils [24]. The flexibility of the N-terminal region is also indicated by the solid-state NMR study of Aβ-(1–42) amyloid fibrils [21]. Our results are also consistent with the structure of Aβ amyloid fibrils, where each molecule associates in a parallel fashion [21,25,26].

It has been demonstrated that Aβ-(1–40) and Aβ-(1–42) are co-mixed within fibrils, suggesting that they possess the same structural architecture [27]. Several structural differences, however, have been suggested. Aβ-(1–40) adopts a strand-turn-strand conformation with β-strands at V12–V24 and A30–V40 [25,26]. A similar, but slightly different position of β-strands is suggested for Aβ-(1–42), in which the strands are composed of V18–S26 and I31–A42 [21]. In the present study, a dramatic decrease in peak intensity was observed in the C-terminal region, whereas G38–V40 exhibited a moderate decrease (Fig. 3). This implies that the G38–V40 region of Aβ-(1–40) is flexible and does not tightly interact with the Aβ-(1–42) seed. The flexible motion of Aβ-(1–40) at the C-terminal would be derived from the structural differences between Aβ-(1–40) and Aβ-(1–42) amyloid fibrils. Such differences

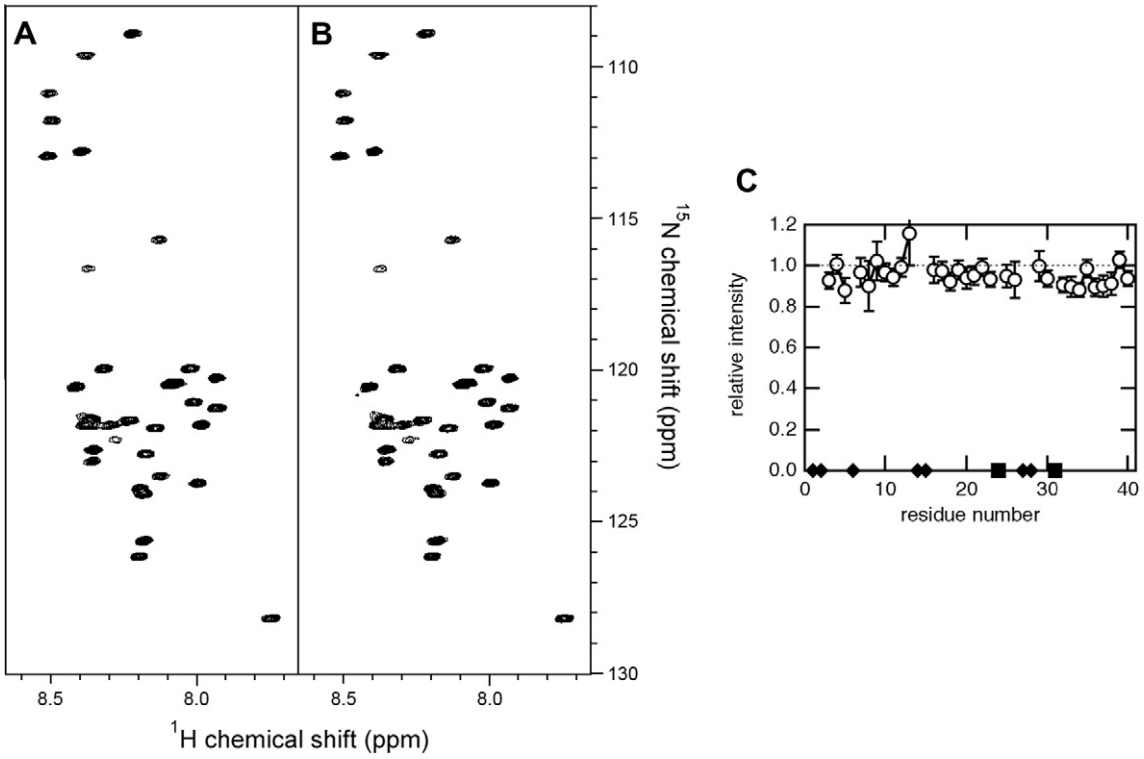

Fig. 5. ^{1}H–^{15}N HSQC spectra of 75 μM ^{15}N-Aβ-(1–40) in the absence (A) and presence of 1 μM spin-labeled A30C-Aβ-(1–42) monomer (B). Peak intensity of ^{15}N-Aβ-(1–40) in the presence of A30C-labeled monomer relative to that in the absence of spin-labeled species is plotted against residue number (C). Definitions of closed diamonds and squares are the same as in Fig. 3.

may eventually lead to the long lag phase in the elongation kinetics of Aβ-(1–40) monomers seeded with Aβ-(1–42) fibrils.

Fawzi et al. [28] examined the exchange reaction between Aβ monomers and protofibrils by using ^{15}N dark-state exchange saturation transfer. They demonstrated that a simple two-state model with a monomer-protofibril failed to reproduce the experimental DEST-profile, and proposed the presence of at least two kinds of bound forms ($I_{contact}$ and $I_{tethered}$). This model is considered to be a residue-specific expansion of the Dock-Lock model. They showed that the residue-specific equilibrium constant ($K3 = [I_{contact}]/[I_{tethered}]$) was significantly larger in the central hydrophobic region and part of the C-terminal region, indicating these regions are in direct contact with the protofibril surface. They also showed that the $^{15}N - R_2^{thethered}$ values of the C-terminal residues in Aβ-(1–40) were small, indicating these residues are highly dynamical in the tethered state. Although the experimental conditions differed between their study and the present study (protofibril vs sonicated fibril seed, homogenous vs heterogeneous), both studies suggest that the center to C-terminal region is responsible for the interaction with fibrils.

In this study, we investigated the mechanisms by which Aβ-(1–40) elongates from preformed Aβ-(1–42) seeds. When Aβ-(1–42) seed was added to seed-free Aβ-(1–40), the aggregation profile exhibited a lag phase. The PRE analysis showed that the Aβ-(1–40) monomer and Aβ-(1–42) seed interact mainly via their C-terminal region. The C-terminal region of Aβ-(1–42) would be a promising therapeutic target for inhibiting Aβ aggregation.

Acknowledgment

This work was supported by the Research Funding for Longevity Sciences (22-14) from National Center for Geriatrics and Gerontology (NCGG), Japan.

References

[1] Hardy, J. and Selkoe, D.J. (2002) The amyloid hypothesis of Alzheimer's disease: progress and problems on the road to therapeutics. Science 297, 353–356.
[2] Selkoe, D.J. (1994) Cell biology of the amyloid β-protein precursor and the mechanism of Alzheimer's disease. Annu. Rev. Cell Biol. 10, 373–403.
[3] Jarrett, J.T., Berger, E.P. and Lansbury Jr., P.T. (1993) The carboxy terminus of the β amyloid protein is critical for the seeding of amyloid formation: implications for the pathogenesis of Alzheimer's disease. Biochemistry 32, 4693–4697.
[4] Zou, K., Kim, D., Kakio, A., Byun, K., Gong, J.S., Kim, J., Kim, M., Sawamura, N., Nishimoto, S., Matsuzaki, K., Lee, B., Yanagisawa, K. and Michikawa, M. (2003) Amyloid β-protein (Aβ)1–40 protects neurons from damage induced by Aβ1–42 in culture and in rat brain. J. Neurochem. 87, 609–619.
[5] Jarrett, J.T. and Lansbury Jr., P.T. (1992) Amyloid fibril formation requires a chemically discriminating nucleation event: studies of an amyloidogenic sequence from the bacterial protein OsmB. Biochemistry 31, 12345–12352.
[6] Jarrett, J.T. and Lansbury Jr., P.T. (1993) Seeding "one-dimensional crystallization" of amyloid: a pathogenic mechanism in Alzheimer's disease and scrapie? Annu. Rev. Cell Biol. 73, 1055–1058.
[7] Naiki, H. and Nakakuki, K. (1996) First-order kinetic model of Alzheimer's β-amyloid fibril extension in vitro. Lab. Invest. 74, 374–383.
[8] Naiki, H. and Gejyo, F. (1999) Kinetic analysis of amyloid fibril formation. Methods Enzymol. 309, 305–318.
[9] Esler, W.P., Stimson, E.R., Jennings, J.M., Vinters, H.V., Ghilardi, J.R., Lee, J.P., Mantyh, P.W. and Maggio, J.E. (2000) Alzheimer's disease amyloid propagation by a template-dependent dock-lock mechanism. Biochemistry 39, 6288–6295.
[10] Yamaguchi, T., Yagi, H., Goto, Y., Matsuzaki, K. and Hoshino, M. (2010) A disulfide-linked amyloid-β peptide dimer forms a protofibril-like oligomer through a distinct pathway from amyloid fibril formation. Biochemistry 49, 7100–7107.
[11] Yamaguchi, T., Matsuzaki, K. and Hoshino, M. (2011) Transient formation of intermediate conformational states of amyloid-β peptide revealed by heteronuclear magnetic resonance spectroscopy. FEBS Lett. 585, 1097–1102.
[12] Murakami, K., Irie, K., Morimoto, A., Ohigashi, H., Shindo, M., Nagao, M., Shimizu, T. and Shirasawa, T. (2002) Synthesis, aggregation, neurotoxicity, and secondary structure of various Aβ1–42 mutants of familial Alzheimer's disease at positions 21–23. Biochem. Biophys. Res. Commun. 294, 5–10.
[13] Delaglio, F., Grzesiek, S., Vuister, G.W., Zhu, G., Pfeifer, J. and Bax, A. (1995) NMRPipe: a multidimensional spectral processing system based on UNIX pipes. J. Biomol. NMR 6, 277–293.
[14] Garrett, D.S., Powers, R., Gronenborn, A.M. and Clore, G.M. (1991) A common sense approach to peak picking in two, three and four-dimensional spectra using automatic computer analysis of contour diagrams. J. Magn. Reson. 95, 214–220.
[15] Hasegawa, K., Yamaguchi, I., Omata, S., Gejyo, F. and Naiki, H. (1999) Interaction between Aβ(1–42) and Aβ(1–40) in Alzheimer's β-amyloid fibril formation in vitro. Biochemistry 38, 15514–15521.
[16] Jan, A., Gokce, O., Luthi-Carter, R. and Lashuel, H.A. (2008) The ratio of monomeric to aggregated forms of Aβ40 and Aβ42 is an important determinant of amyloid-β aggregation, fibrillogenesis, and toxicity. J. Biol. Chem. 283, 28176–28189.
[17] Pauwels, K., Williams, T.L., Morris, K.L., Jonckheere, W., Vandersteen, A., Kelly, G., Schymkowitz, J., Rousseau, F., Pastore, A., Serpell, L.C. and Broersen, K. (2011) The structural basis for increased toxicity of pathological Aβ42:Aβ40 ratios in Alzheimer's disease. J. Biol. Chem. 287, 5650–5660.
[18] Chatani, E., Lee, Y.H., Yagi, H., Yoshimura, Y., Naiki, H. and Goto, Y. (2009) Ultrasonication-dependent production and breakdown lead to minimum-sized amyloid fibrils. Proc. Natl. Acad. Sci. USA 106, 11119–11124.
[19] O'Nuallain, B., Shivaprasad, S., Kheterpal, I. and Wetzel, R. (2005) Thermodynamics of Aβ(1–40) amyloid fibril elongation. Biochemistry 44, 12709–12718.
[20] Yan, Y. and Wang, C. (2007) Aβ40 protects non-toxic Aβ42 monomer from aggregation. J. Mol. Biol. 369, 909–916.
[21] Ahmed, M., Davis, J., Aucoin, D., Sato, T., Ahuja, S., Aimoto, S., Elliott, J.I., Van Nostrand, W.E. and Smith, S.O. (2010) Structural conversion of neurotoxic amyloid-$\beta_{(1-42)}$ oligomers to fibrils. Nat. Struct. Mol. Biol. 17, 561–567.
[22] Lührs, T., Ritter, C., Adrian, M., Riek-Loher, D., Bohrmann, B., Döbeli, H., Schubert, D. and Riek, R. (2005) 3D structure of Alzheimer's amyloid-β(1–42) fibrils. Proc. Natl. Acad. Sci. USA 102, 17342–17347.
[23] Masuda, Y., Uemura, S., Nakanishi, A., Ohashi, R., Takegoshi, K., Shimizu, T., Shirasawa, T. and Irie, K. (2008) Verification of the C-terminal intramolecular β-sheet in Aβ42 aggregates using solid-state NMR: implications for potent neurotoxicity through the formation of radicals. Bioorg. Med. Chem. Lett. 18, 3206–3210.
[24] Olofsson, A., Lindhagen-Persson, M., Sauer-Eriksson, A.E. and Öhman, A. (2007) Amide solvent protection analysis demonstrates that amyloid-β(1–40) and amyloid-β(1–42) form different fibrillar structures under identical conditions. Biochem. J. 404, 63–70.
[25] Petkova, A.T., Ishii, Y., Balbach, J.J., Antzutkin, O.N., Leapman, R.D., Delaglio, F. and Tycko, R. (2002) A structural model for Alzheimer's β-amyloid fibrils based on experimental constraints from solid state NMR. Proc. Natl. Acad. Sci. USA 99, 16742–16747.
[26] Petkova, A.T., Yau, W.-M. and Tycko, R. (2006) Experimental constraints on quaternary structure in Alzheimer's β-amyloid fibrils. Biochemistry 45, 498–512.
[27] Török, M., Milton, S., Kayed, R., Wu, P., McIntire, T., Glabe, C.G. and Langen, R. (2002) Structural and dynamic features of Alzheimer's Aβ peptide in amyloid fibrils studied by site-directed spin labeling. J. Biol. Chem. 277, 40810–40815.
[28] Fawzi, N.L., Ying, J., Ghirlando, R., Torchia, D.A. and Clore, G.M. (2011) Atomic-resolution dynamics on the surface of amyloid-β protofibrils probed by solution NMR. Nature 480, 268–272.